

1 **Composite Bi-layered Erodible Films for Potential Ocular Drug Delivery**

2 J.S. Boateng^{1*}, A.M. Popescu¹

3 ¹Department of Pharmaceutical, Chemical and Environmental Sciences, Faculty of
4 Engineering and Science, University of Greenwich, Medway, UK, ME4 4TB

5
6 *Correspondence: Dr Joshua Boateng (j.s.boateng@gre.ac.uk; joshboat40@gmail.com)

27 **Abstract**

28 Bi-layered hydroxypropylmethylcellulose and Eudragit based films were formulated as
29 potential ocular drug delivery systems using chloramphenicol as a model antibiotic. Films were
30 plasticized with polyethylene glycol 400 present in the Eudragit layer or both Eudragit and
31 hydroxypropylmethylcellulose layers, and loaded with chloramphenicol (0.5% w/v in solution)
32 in the hydroxypropylmethylcellulose layer. The weight, thickness and folding endurance
33 optimized formulations were measured and further characterized for transparency, tensile,
34 mucoadhesive, swelling and *in vitro* drug dissolution properties. The physical form of
35 chloramphenicol within the films was evaluated using differential scanning calorimetry (DSC),
36 and X-ray diffraction (XRD), complimented with scanning electron microscopy and energy
37 dispersive X-ray spectroscopy. Fourier transform infrared spectroscopy was used to assess the
38 interactions between the drug and the film components and confirm chloramphenicol's
39 presence within the sample. Optimum films showed high transparency ($\geq 80\%$ transmittance),
40 ease of peeling from Petri dish and folding endurance above 250. Average thickness was lower
41 than contact lenses (0.4 - 1mm), confirming them as thin ocular films. The tensile properties
42 showed a good balance between toughness and flexibility and mucoadhesivity showed that
43 they could potentially adhere to the ocular surface for prolonged periods. The drug loaded films
44 showed swelling capacity which was greater than 300% of their original weight. The physical
45 form of chloramphenicol within the films was amorphous (DSC and XRD) whilst *in vitro* drug
46 dissolution showed sustained drug release from the films for four hours, before complete
47 erosion. The chloramphenicol loaded films represent a potential means of treating common eye
48 infections.

49
50 **Keywords:** Antibacterial, bi-layered films, mucoadhesion, *in vitro* drug release, ocular
51 delivery, plasticizer.

52 **1 Introduction**

53 Vision provides 90% of the information within our surrounding environment, with
54 considerable physiological importance including differentiation between light, shape and
55 colour, spatial orientation, equilibrium and cortical tone [1]. Various conditions can affect the
56 eyes and these are classified as periocular and intraocular, according to their location.
57 Periocular conditions occur around the eye and can cause irritation to different parts of the eye.
58 Common periocular diseases include blepharitis, conjunctivitis and chronic conditions caused
59 by bacteria which can even lead to vision impairment [2]. Effective reduction of bacterial load
60 is very important in the treatment of ocular diseases caused by infection.

61 The development of ocular drug delivery systems is challenging because of the eyes'
62 complex anatomic structure and protective mechanisms which make it difficult to maintain an
63 effective drug concentration over a prolonged period of time [3-8]. The eye is a very sensitive
64 organ to debris, microorganisms and drugs and therefore, ocular drug delivery systems should
65 be simple, non-invasive (to prevent irritation, inflammation, infection), maintain visual clarity,
66 and enable the drug to penetrate the physiological eye barriers to reach the site of action [9].

67 Ocular drug delivery for treating conditions affecting the front of the eye depends on the
68 corneal barrier and tear film. Apart from the physiological factors, there are also factors
69 affecting formulation development, of ophthalmic preparations including osmolality, pH,
70 surface tension and viscosity [10].

71 Topical eye drops represent the most convenient formulation among patients, especially
72 for conditions affecting the anterior segment of the eye. However, only 5% of the instilled dose
73 can penetrate the ocular pre-corneal, dynamic and static barriers, while constant and prolonged
74 drug release cannot be achieved [11]. Though gels and ointments can remain for relatively
75 longer periods, they are quickly diluted by the tear fluid and leak out, therefore reducing
76 bioavailability [12]. Ocular inserts such as films have been developed, which are expected to

77 maintain the drug on the eye surface for a relatively prolonged period better than drops, gels
78 and ointments. These increase the contact time with the ocular surface and therefore prolong
79 drug delivery, reduce systemic effects, improve patient compliance and increase bioavailability
80 [12].

81 Erodible films are made of polymers that can be natural, synthetic or semi-synthetic and
82 that provide support for loaded drug. The polymers used need to be bio-compatible, safe, non
83 reactive, stable and mucoadhesive, and release drug appropriately [13]. The drugs contained
84 within the films are usually in the form of a dispersion within the matrix whilst maintaining
85 film clarity [14]. Acyclovir, phenylephrine, diclofenac sodium, and antibiotics are examples
86 of drugs that can be contained within the ocular inserts. All drugs need an appropriate balance
87 between lipid and water solubility for effective corneal permeation. In addition, films generally
88 need a plasticiser to improve their flexibility and reduce the chances of contact irritation due
89 to britleness.

90 In the present study, bi-layered erodible ocular films were prepared by solvent casting
91 technique from solutions using hydrophobic Eudragit (EUD) and hydrophilic
92 hydroxypropylmethylcellulose (HPMC). These polymers are safe and biocompatible, stable,
93 mucoadhesive and provide sustained drug release *in vitro*, making them suitable for ocular
94 delivery [15]. Polyethylene glycol 400 was used as a plasticiser in either the EUD or both
95 polymeric layers to increase the flexibility of the films.

96 Chloramphenicol (CHF) was used as model drug and exhibits broad-spectrum
97 antibacterial activity [16] against Gram-positive bacteria (*Staphylococcus aureus* and,
98 *Streptococcus pyogenes*) and Gram-negative bacteria *Haemophilus influenza* and *Neisseria*
99 *meningitides*) common in ocular infections such as conjunctivitis [17]. Due to its high
100 lipophilicity, CHF can easily penetrate the ocular barriers, and therefore very effective against
101 ocular infections [17] However, its high lipid solubility facilitates easy absorption into the

102 systemic circulation and side effects such as aplastic anaemia can occur with prolonged
103 exposure. Therefore, CHF is safely and efficiently used in eye drops at of 0.5% w/v
104 (approximately 5000µg/ml) this dose was employed in this study [18]. The MIC values of CHF
105 against the above organisms range from 0.25 - 128µg/ml [19] which is far lower than the dose
106 used in this study. Because the residence time of eye drops on the cornea is poor, the use of the
107 0.5% CHF dose within a mucoadhesive film which can prolong retention on the cornea and
108 control drug release, is expected to overcome limitation of the former. Further, a more gradual
109 release of CHF which prevents frequent administration, will reduce the incidence of side effects
110 associated with CHF.

111

112 **2 Experimental**

113 *2.1 Materials*

114 Eudragit S100 (EUD) was obtained from Degussa (Germany),
115 hydroxypropylmethylcellulose – HPMC (Methocel™ K100 Premium) was a gift from
116 Colorcon Limited (Dartford, UK). PEG, methanol, absolute ethanol, acetone, isopropyl
117 alcohol, acetonitrile (HPLC grade) and phosphoric acid (HPLC grade) were supplied from
118 Fisher Scientific, (Leicestershire, UK). Chloramphenicol was obtained from Sigma-Aldrich
119 (Gillingham, UK). Sodium chloride, potassium chloride, sodium phosphate dibasic anhydrous
120 (99+ % extra pure) and potassium phosphate dibasic anhydrous (99+ % extra pure) were all
121 obtained from Acros Organics Ltd (New Jersey, USA).

122

123 *2.2 Film formulation development*

124 Different ratios of EUD to HPMC were weighed and dissolved in different mixtures of
125 water with acetone, isopropyl alcohol, ethanol and methanol to obtain the polymeric solutions.
126 However, none of the mixtures resulted in a completely clear film due to the poor water

127 solubility of EUD. The development of a completely clear EUD film was therefore achieved
 128 for a 2% w/v solution by dissolving the polymer in a mixture of acetone and isopropyl alcohol
 129 (ratio 3:2). HPMC only solution (2% w/v) was obtained by dissolving the required amount of
 130 polymer in deionised water. Bi-layered blank (BLK) films were subsequently prepared using
 131 the two 2% w/v (HPMC and EUD) solutions.

132 Table 1 Preparation of (a) solutions (2% w/v) required for BLK HPMC-EUD and (b)
 133 solutions (2% w/v) required for DL HPMC-EUD; bi-layered film formation.

134 (a)

EUD film				
	Polymer (g)	PEG (g)	Acetone (ml)	Isopropyl alcohol (ml)
EUD 1	2.007	2.001	60	40
EUD 2	2.005	1.001	60	40
HPMC film				
	Polymer (g)	PEG used (g)	CHF (g)	Deionized water (ml)
HPMC 1	2.002	-	-	100
HPMC 2	2.005	1.002	-	100

135 (b)

136

137

EUD film				
	Polymer (g)	PEG (g)	Acetone (ml)	Isopropyl alcohol (ml)
EUD 3	2.007	2.001	60	40
EUD 4	2.001	1.002	60	40
HPMC films				
	Polymer (g)	PEG (g)	CHF (g)	Deionised water (ml)
HPMC 3	2.000	-	0.50	100
HPMC 4	2.004	1.001	0.50	100

138

139 Subsequently, 10g of the HPMC solution was poured onto the water insoluble EUD
140 films and left to dry at room temperature for a further 24 hours to obtain the final bi-layered
141 film. The drug loaded (DL) bi-layered films were obtained as above but with CHF (0.5% w/v)
142 loaded in the HPMC solution before pouring on the BLK EUD film. For plasticised films, PEG
143 (1.0% w/v) was added into either the EUD only or split between EUD (0.5% w/v) and HPMC
144 (0.5% w/v) solutions. After preparation, 10g of EUD solution was poured into glass a Petri dish
145 (82mm diameter) and left at room temperature for 24 hours to obtain the first film layer. The
146 BLK (HPMC-EUD-PEG & HPMC-PEG-EUD-PEG) and DL (HPMC-CHF-EUD-PEG &
147 HPMC-PEG-CHF-EUD-PEG) films (Table 1) were peeled from the Petri dish, visually
148 examined for any physical defects (e.g. patches, scratches, cracks and tears) and suitable films
149 stored in desiccators over silica until ready for use.

150 151 *2.3 Physical measurements*

152 *2.3.1 Film thickness and weight*

153 Three film samples ($n = 3$) from each formulation were cut into 20 x 20mm² strips, individually
154 weighed using a digital balance and average weight per mm² calculated. Thickness was
155 measured using a Metric micrometre screw gauge at five different locations i.e. four corners
156 and middle and the average thickness calculated [20].

157 158 *2.3.2 Transparency test*

159 Light transmittance was measured using a spectrophotometer (Model U-2900) set between the
160 UV and IR range (300-1100nm). A 40 x 10mm² strip was cut from each formulation and
161 introduced into the spectrophotometer cell and percentage transmittance measured at a scan
162 speed of 400nm/min.

163

164 2.3.3 *Folding endurance*

165 A whole film removed from the Petri dish was used. Folding endurance was measured by
166 repeatedly folding the film longitudinally at the same place until it broke [21], but no more
167 than 250 times and recorded.

168

169 2.4.1 *Texture analysis*

170 2.4.1 *Mechanical (tensile) properties*

171 The tensile properties (% elongation at break, tensile strength and elastic modulus) were
172 measured using a TA.HD.*plus* Texture Analyser (Stable Micro Systems, Surrey, UK) equipped
173 with a 5kg load cell. Films were cut into 50 x 10mm² rectangular strips and their thickness
174 measured. Each strip was held between the tensile grips of a texture analyser positioned 30mm
175 apart. The strips were pulled using a trigger force of 0.09N at a crosshead speed of 0.1mms⁻¹
176 until they broke. The tensile properties were calculated using equations 1 - 3.

177

178
$$\text{Tensile strength} = \frac{\text{Force at failure}}{\text{cross-sectional area of the film}} \quad \text{Equation (1)}$$

179

180
$$\text{Percent elongation at break} = \frac{\text{Increase in length at break}}{\text{Initial film length}} \times 100 \quad \text{Equation (2)}$$

181

182
$$\text{Elastic modulus} = \frac{\text{Slope of stress-strain curve}}{\text{Film thickness} \times \text{Cross head speed}} \quad \text{Equation (3)}$$

183

184 2.4.2 *In vitro mucoadhesion*

185 Each formulation was cut into four 10 x 10mm² strips and attached onto the adhesive
186 probe of a texture analyser equipped with a 5kg load cell, using double-sided adhesive tape. A
187 model mucosa substrate in a Petri dish (86mm diameter), formed from a 6.67% w/v gelatine
188 solution, allowed to set to form a solid gel, was equilibrated by spreading 20µl PBS solution

189 (pH 7.4) over its surface to simulate the ocular mucosa. The film attached to the probe was
190 pressed onto the gelatine surface at a force of 0.5N, for 120 seconds (to allow proper contact
191 with the gelatine layer) and detachment initiated [22]. The mucoadhesion strength was
192 measured as the maximum force (F_{max}) required for detaching the sample from the gelatine
193 surface [23].

194

195 *2.5 Scanning electron microscopy (SEM)*

196 SEM was used to analyse the surface morphology of the BLK and DL bi-layered films.
197 Two small strips (0.5 x 0.5cm²) were cut from each film, attaching to a sample holder and
198 coating with chromium to make them conductive and protect from heat. Both EUD and HPMC
199 layers were analysed, to observe differences in morphology. The images were acquired using
200 a Hitachi SU8030 scanning electron microscope with electronic beam voltage of 1.0kV,
201 working distance of 8mm at different magnifications (x 250, 1000, 5000 and 10000).

202

203 *2.6 Analytical characterisation*

204 *2.6.1 Attenuated total reflectance Fourier transform infrared (ATR-FTIR) spectroscopy*

205 FTIR spectroscopy was used to analyse the presence of CHF in the DL films as well as
206 the chemical interactions between the drug and the polymers. Testing was performed on a
207 Perkin Elmer ATR-FTIR machine (Model Spectrum Two), at a wavelength between 450 and
208 4000cm⁻¹. The BLK and DL films, and starting materials were analysed. Prior to sample
209 analyses, a background scan was performed and subtracted from all sample spectra.

210

211 2.6.2 *Differential scanning calorimetry (DSC)*

212 DSC was used to assess the thermal behaviour of the BLK and DL films, and pure CHF.

213 A small sample (2-5mg) was placed into a 40 μ l aluminium pan and sealed hermetically. The

214 samples were heated between 25°C and 250°C at a rate of 10°C/min.

215

216 2.6.3 *X-ray diffraction (XRD)*

217 XRD was used to determine the physical form of BLK and DL films and CHF. The films

218 were cut into six pieces and placed on top of each other in the transmitter holder. The samples

219 were analyzed at an angular range of 4-45° 2 θ , rotation of 15rpm and 0.6mm exit slit at

220 increments of 0.02° 2 θ [24].

221

222 2.6.4 *Energy dispersive x-ray (EDX) spectroscopy*

223 A Hitachi SU8030 SEM equipped with a Thermo Fisher Scientific EDX was used to

224 analyse the energy spectrum of the samples. The analysis was performed at an accelerating

225 voltage of 8kV, working distance of 8mm and magnification of x9020, in order to determine

226 the chlorine atoms present on the surface of the DL films and therefore demonstrate the

227 distribution of CHF.

228

229 2.7 *Swelling capacity*

230 Swelling test was carried out to measure the swelling capacity of the optimum BLK and

231 DL films. The films were cut into 20 x 20mm² square strips and weighed accurately. Each strip

232 was immersed into a Petri dish containing 5ml PBS solution at pH 7.4 and incubated at

233 37 \pm 0.5°C [25]. At specific time intervals (10 minutes), the films were removed, blotted

234 carefully with tissue paper to remove the excess PBS solution and accurately weighed. Then

235 5ml of PBS solution was added to the previously swollen film and the procedure repeated till

236 no more increase in weight was observed. The swelling capacity (Q_s) was calculated for each
237 time point using equation 4.

$$238 \quad Q_s = \frac{W_t - W_0}{W_0} \times 100 \quad \text{Equation (4)}$$

239 Where, W_t is the weight of the swollen sample and W_0 is the weight of the dried film.

240

241 *2.8 In vitro drug dissolution studies*

242 Prior to drug dissolution studies, HPLC was performed on an Agilent 1200 instrument,
243 equipped with an auto sampler, using a 150mm × 4.6mm × 5µm column. The mobile phase
244 comprised acetonitrile, deionised water and phosphoric acid – in volume ratio of 65: 35: 0.1
245 with flow rate of 1.0ml/min and detection wavelength set at 280nm. Initially, standard solutions
246 0.05, 0.10, 0.15, 0.20 and 0.25mg/ml of CHF in PBS solution (pH 7.4) were used to plot a
247 calibration graph ($R^2 = 0.997$) and used to calculate % drug release. For the drug dissolution
248 studies, each DL film was cut into 20 × 20mm² strips, weighed and placed in 20ml PBS, in a
249 Petri dish. At pre-determined time intervals (0, 15, 30, 45, 60, 90, 120, 150, 180, 240 and 300
250 minutes), 1.0ml aliquots were removed from each Petri dish and replaced with 1.0ml of fresh
251 medium. The sampled solutions were analysed by HPLC as above.

252

253 **3 Results and discussion**

254 Ocular drug delivery systems need to possess functional characteristics such as being simple,
255 non-invasive, maintaining visual clarity, allowing prolonged residence of the drug on the eye,
256 to penetrate the physiological eye barriers and reach the site of action [9].

257

258 *3.1 Formulation development and optimisation*

259 Bi-layered, erodible HPMC and EUD films containing CHF were successfully
260 developed and tested. These two polymers are well characterised for safety and

261 biocompatibility and known to be stable under normal processing and storage conditions. The
262 2% w/v EUD and HPMC solutions used to prepare films were easy to handle and no heat was
263 required during their formation. EUD only films were too thin, and difficult to remove from
264 the Petri dish, but the addition of an HPMC solution layer on top of the EUD film led to the
265 formation of a bi-layered film that was easy to peel from the Petri dish. Unplasticised films
266 were brittle and addition of PEG made them more flexible and transparent. Figure 1 shows
267 digital images of the four optimum bi-layered (two BLK and two DL) formulations selected
268 for further testing.

269

270 *3.2 Physical measurements*

271 *3.2.1 Thickness and film weight*

272 The thickness and weight of the optimized BLK and DL HPMC-EUD-PEG- and HPMC-PEG-
273 EUD-PEG were measured. The average thickness of the films was between 12 and 17 μ m,
274 which classifies them as thin ocular films, and expected to be comfortable to the eyes **Error!**
275 **Reference source not found.** Further, the weight/mm² increased as more components (PEG
276 and CHF) were added to the HPMC solution layer. The starting weight/mm² for the BLK
277 HPMC-EUD-PEG film was 14.5, which increased by 15.51% after the addition of PEG within
278 the HPMC layer, 6.89% after the addition of drug and by 29.31% after the addition of both
279 plasticiser and drug.

280

281 *3.2.2 Transparency test*

282 An effective ocular formulation is expected not to interfere with sight and vision of the patient
283 to avoid non-compliance [27], therefore in addition to visual observation, transmittance was
284 recorded to determine the transparency of the BLK and DL films. Within the visible spectrum
285 (400 and 700nm), the light transmittance of all samples was above 80% and no major peak was

286 present within this range. The BLK and DL films with only the EUD layer plasticised (HPMC-
287 EUD-PEG and HPMC-CHF-EUD-PEG respectively) had approximately 80% light
288 transmission, while the BLK and DL films with both layers plasticised (HPMC-PEG-EUD-
289 PEG and HPMC-PEG-CHF-EUD-PEG) was higher at 87.5%. Therefore, drug loading did not
290 appear to significantly affect the clarity of the samples, whilst the addition of PEG in the
291 formulation of both HPMC and EUD solutions led to a higher transparency, making plasticised
292 films more suitable for ocular drug delivery. Though the films were clear when observed
293 visually, further improvement of transparency to 96%, to match that of contact lenses, will be
294 ideal **Error! Reference source not found.** This may be achieved by the addition of more
295 plasticiser in both polymeric layers.

296

297 *3.2.3 Folding endurance*

298 Optimized BLK and DL films were longitudinally folded at the same place to assess their
299 resistance to folding during repeated handling. None of the films broke after being folded 250
300 times, implying good resistance to handling, which is an essential functional characteristic for
301 any ocular drug delivery system which must be safe to the patient if it needs to be removed and
302 reinserted [29] while remaining intact. The folding endurance is also an indication of
303 mechanical resistance to deformation, however, to more accurately determine the mechanical
304 properties of the films, tensile properties were measured using a texture analyser.

305

306 *3.3 Texture analysis*

307 *3.3.1 Mechanical (tensile) properties*

308 The tensile properties (tensile strength, elastic modulus and % elongation at break) of the BLK
309 and DL EUD-HPMC films are shown in Figure 2a. All the films had % elongation values
310 within the reported ideal range of 30 – 50% [30] where films are neither too brittle nor too

311 sticky, which is important to avoid breaking or difficulty in handling. The highest value for
312 elastic modulus was achieved by the BLK HPMC-EUD-PEG films. The values of elastic
313 modulus showed that addition of PEG in both EUD and HPMC layers made the films more
314 flexible, which was also confirmed by the higher values of % elongation at break for these
315 films. Addition of CHF made them more flexible with HPMC-PEG-CHF-EUD-PEG having
316 better tensile properties compared to HPMC-CHF-EUD-PEG film due to the addition of PEG
317 in both polymeric layers of the former. This resulted in better elasticity, decreased stiffness and
318 brittleness, making it more suitable for ocular drug delivery as its flexibility makes it less likely
319 to cause contact irritation, therefore potentially providing better patient compliance [31].
320 Plasticisers generally act by interrupting the intermolecular interactions between polymer
321 chains and increasing the specific volume, thus increasing their molecular mobility and
322 therefore making them more flexible [32].

323 324 *3.3.2 In vitro mucoadhesion studies*

325 Mucoadhesion strength was measured using the gelatine layer, to simulate bioadhesion of the
326 films to the ocular surface. As shown in Figure 2b, the highest detachment force necessary to
327 remove the film from the gelatine layer was observed for BLK and DL films with only the
328 EUD layer plasticised (HPMC-EUD-PEG and HPMC-CHF-EUD-PEG). This is interesting and
329 appears to confirm the swelling capacity results below. This is because the initial stages of
330 mucoadhesion involve polymer hydration and swelling which enhance the inter-diffusion
331 process, allowing physical entanglement and enhanced surface availability for hydrogen
332 bonding and electrostatic interaction between the polymeric chains and the model mucosal
333 substrate.

334 Overall, the average detachment force required for all samples was higher than the force
335 (0.2N) required by the eyelids to blink, implying that the formulated films will not be easily

336 dislodged by blinking. In addition, due to their thin nature, the hydrated ocular films are
337 expected to be comfortable to patients though this will need to be confirmed in an *in vivo* study.

338 *3.4 Scanning electron microscopy (SEM)*

339 The SEM images for CHF confirmed its crystalline structure, as shown in Figure 3a.
340 The images obtained from the surface of both sides of the BLK films, shown in the Figure 3 (b
341 & c) revealed the presence of flat and irregular three-dimensional crystals on the surface of the
342 HPMC layer. These may be due to the incomplete dissolution of HPMC in water, or the slow
343 drying process at room temperature, which allowed some of the dissolved polymer to
344 recrystallize on the surface as HPMC is known to be semi-crystalline. The EUD layer was
345 smooth, possibly due to the complete dissolution of the polymer in organic solvents during
346 formulation. The SEM images obtained for the surface of the DL HPMC-EUD films shown in
347 Figure A1 (d – g) of the appendix revealed the presence of needle shaped structures, which
348 may be CHF crystals. The EUD layer remained smooth, confirming the possibility of complete
349 dissolution of EUD within the acetone and isopropyl alcohol.

350 SEM of the HPMC layer of DL films appears to contradict the results from DSC and
351 XRD testing, which showed that the drug was possibly changed to its amorphous form or
352 molecularly dispersed during the formulation process. Further analysis of the needle-shaped
353 crystals was therefore necessary in order to determine whether they represent another
354 crystalline form of CHF, and this was done using EDX analysis.

355

356 *3.5 Analytical characterisation*

357 *3.5.1 Fourier transform infrared spectroscopy (FTIR)*

358 The FTIR spectra obtained for the BLK and DL films are shown in Figure A2 of the
359 appendix, showing similar peak patterns, due to similar formulation components (HPMC and
360 EUD). The peak present around 3500cm^{-1} is attributed to the presence of the OH group of

361 HPMC. The C=O group of EUD was observed around 1750cm^{-1} and the peaks present around
362 1000cm^{-1} is due to the presence of the C-O bond, from HPMC and EUD. The addition of PEG
363 in both polymeric layers and of CHF resulted in additional sharp peaks. A peak was observed
364 at 1522cm^{-1} for only DL films, and attributed to the aromatic ring present in CHF, suggesting
365 little or no interaction between the drug and the polymer within the HPMC layer.

366

367 *3.5.2 Differential scanning calorimetry (DSC)*

368 Figure 4 shows the DSC thermograms obtained for CHF and BLK and DL bi-layered
369 HPMC-EUD films. The sharp peak for pure CHF (Figure 4a) revealed its crystalline nature and
370 its melting point matched that previously reported at 159.06°C [33]. The thermograms for the
371 BLK and DL films (Figure 4b) showed no obvious sharp peaks expected for crystalline
372 materials, suggesting that CHF was converted to the amorphous form or molecularly dispersed
373 within the polymeric matrix. It is also possible that the amount of CHF present in the small 2-
374 5mg sample analysed was too low to allow detection. The BLK films showed a broad
375 endothermic peak beyond 210°C which was not found in the corresponding DL films. This
376 might relate to the presence of free PEG which was not available in the DL films due to the
377 presence of CHF.

378

379 *3.5.3 X-ray diffraction (XRD)*

380 XRD diffractograms for the BLK and DL films are shown in Figure 5a. The
381 diffractogram obtained for CHF (data not shown) clearly showed its crystalline nature with
382 sharp peaks comparable with reference peaks in the instrument database. For the BLK HPMC-
383 EUD film samples, the diffractograms showed a typically amorphous pattern with a broad peak.
384 The analysis of the DL HPMC-EUD films gave similar results, confirming the DSC results that

385 the drug was possibly changed to its amorphous form or molecularly dispersed during film
386 formulation.

387

388 *3.5.4 Energy dispersive x-ray spectroscopy (EDX)*

389 EDX spectroscopy confirmed the presence of chlorine and nitrogen atoms within pure
390 CHF. However, it did not confirm the presence of the drug in the DL film, as no chlorine or
391 nitrogen atoms were detectable (Figure 5b). This may be due to the low amount of CHF within
392 the small section of the films cut for analysis, which was therefore not detectable, or possibly
393 due to the fact that the molecular dispersion of CHF within the polymer matrix caused the
394 chlorine and nitrogen atoms to be shielded by significantly high amounts of polymer chains
395 surrounding them.

396

397 *3.6 Swelling capacity*

398 The initial hydration and swelling of a film are important functional characteristics as they
399 significantly affect other important properties such as mucoadhesion and drug release [34]. The
400 results (Figure 6a) showed that HPMC-CHF-EUD-PEG film hydrated and swelled most
401 rapidly, showing a maximum swelling of 557%. The swelling capacity for the DL films
402 (HPMC-PEG-CHF-EUD-PEG and HPMC-CHF-EUD-PEG) were higher compared to the
403 corresponding BLK films. The higher swelling capacity of DL films can be attributed to the
404 release of CHF from the HPMC layer which allowed further ingress of more fluid into the
405 swollen matrix. Comparing the two DL films, the formulation with both layers plasticised
406 remained intact for a longer period of time, representing an optimum ocular drug delivery
407 system. In addition, all films completely disintegrated after 270 minutes, meaning that they are
408 erodible and will be able to provide sustained drug release for at least 4 hours.

409

410 *3.7 In vitro drug dissolution studies*

411 Drug dissolution profiles of both DL HPMC-EUD films loaded with CHF was
412 monitored using PBS (pH 7.4), to simulate the ocular tear fluid. Both DL films had similar

413 drug dissolution profiles (Figure 6b), showing a biphasic release, with an initial phase where
414 approximately 60% of the drug was released from the matrix within the first two hours,
415 followed by a second sustained release phase. The initial 60% released corresponds to 2273 μ g
416 of CHF which is significantly higher than the MIC of the drug required to kill bacteria which
417 cause common eye infections such as conjunctivitis. However, this will require confirmation
418 in a future *in vitro* antibacterial assay. Further, up to 70% of the drug will be released from the
419 polymeric matrix before the film completely erodes. This bi-phasic release make the films
420 suitable ocular drug delivery systems offering sustained release up to 4 hours, until they
421 completely erode, and therefore more efficient against bacteria in comparison with
422 conventional eye drops and ointments. The plasticiser in both polymeric layers was associated
423 with a slightly reduced drug release, due mainly to the interaction between PEG and the
424 polymers suggesting that it might be better to have the PEG present in just one layer.

425 Other studies [35, 36] have reported the use of drug-soaked soft contact lenses to deliver
426 appropriate amounts of drug, however, though these offer an improvement over eye drops, they
427 have limitations. Firstly, drug loading capacity is dependent on equilibrium drug solubility
428 within the lens. Drug diffusion from the stock solution does not happen instantly and requires
429 several hours for complete saturation. Further, drug concentration in the original solution must
430 be higher than the final soaked lens to maintain effective diffusion gradient, resulting in drug
431 being wasted and therefore uneconomical [37]. Finally, the lens will require re-soaking in drug
432 solution after a short period. On the other hand, the erodible films degrade slowly and therefore
433 can remain on the eye for four hours but without the need for removal. More advanced options
434 include imprinted and liposome loaded lenses or films for sustained drug delivery, however,
435 these are more complex to formulate and more likely to be significantly more expensive than
436 eye drops. The bi-layered films are simple and cost effective and therefore an ideal
437 alternative to eye drops.

438 **4 Conclusion**

439 Bi-layered ocular films were successfully prepared using hydrophobic EUD and hydrophilic
440 HPMC. The HPMC-CHF-EUD-PEG film was the most suitable for ocular drug delivery,
441 having good physicochemical properties, providing sustained drug release, expected to
442 maintain the drug on the eye surface for a relatively prolonged period and also expected to
443 completely erode. The DL films have great potential as ocular drug delivery system for treating
444 common eye infections as they are expected to be easy to use, comfortable, and efficient and
445 their removal would not be necessary. However, an antibacterial study of these films is
446 essential to determine the efficiency of CHF against bacteria that affect the eyes.

447

448 **5 References**

- 449 [1] Cristescu, D, Salavastru, C., Voiculescu, B., Niculescu, C. and Carmaciu, R. (2008).
450 *Biologie*. 1st ed. Bucuresti: Corint, 44-48.
- 451 [2] Pflugfelder, S., Karpecki, P. and Perez, V. (2014). Treatment of Blepharitis: Recent
452 Clinical Trials. *The Ocular Surface*, 12(4), 273-284.
- 453 [3] Hermans, K., Van den Plas, D., Kerimova, S., Carleer, R., Adriaensens, P., Weyenberg,
454 W. and Ludwig, A. (2014). Development and characterization of mucoadhesive
455 chitosan films for ophthalmic delivery of cyclosporine A. *International Journal of*
456 *Pharmaceutics*, 472(1-2), 10-19.
- 457 [4] Pahuja, P., Arora, S., Pawar, P. (2012). Ocular drug delivery system: a reference to
458 natural polymers. *Expert Opinion on Drug Delivery*, 9(7), 837–861.
- 459 [5] Nisha, S., Deepak, K. An insight to ophthalmic drug delivery system. (2012).
460 *International Journal of Pharmaceutical Studies Research*, 3(2), 9–13.
- 461 [6] Gaudana, R., Jwala, J., Boddu S.H.S., Mitra, A.K. (2009). Recent perspectives in ocular
462 drug delivery. *Pharmaceutical Research*, 26(5), 1197–1216.

- 463 [7] Rajasekaran, A., Kumaran, K.S.G.A., Preetha, J.P., Karthika, K. (2010). A comparative
464 review on conventional and advanced ocular drug delivery formulations, *International*
465 *Journal of PharmTech Research*, 2(1), 668–674.
- 466 [8] Tangri, P., Khurana, S. (2011). Basics of ocular drug delivery systems. *International*
467 *Journal of Research in Pharmaceutical and Biomedical Sciences*, 2(4), 1541–1552.
- 468 [9] Lai, S., Wang, Y., Hanes, J. (2009). Mucus-penetrating nanoparticles for drug and gene
469 delivery to mucosal tissues. *Advanced Drug Delivery Reviews*, 61(2), 158-171.
- 470 [10] Aulton, M. (2013). *Pharmaceutics: The Science of Dosage Form Design*. 4th ed.
471 Edinburgh: Churchill Livingstone.
- 472 [11] Patel, A. (2013). Ocular drug delivery systems: An overview. *World Journal of*
473 *Pharmacology* 2(2), 47.
- 474 [12] Boateng, JS, Okeke, O., Khan, S. (2015). Polysaccharide Based Formulations for
475 Mucosal Drug Delivery: A Review. *Current Pharmaceutical Design*. 21(33), 4798-
476 4821.
- 477 [13] Kesarwani, R., Harikumar, S., Rana, A., Kashyap, C., Kaur, A. and Seth, N.
478 (2011) Ocular Implants: a novel approach to ocular drug delivery review. *International*
479 *Journal of Drug Formulation and Research*, 2(5), 93-119.
- 480 [14] Gupta, S., Songara, R. and Lokwani, P. (2011). Ocular Inserts: An Overview.
481 *International Journal of Pharmaceutical Research and Development*, 3(6), 141-148.
- 482 [15] Ludwig, A. (2005). The use of mucoadhesive polymers in ocular drug delivery.
483 *Advanced Drug Delivery Reviews*, 57, 1595–1639.
- 484 [16] Fraunfelder, F., Fraunfelder, F. (2013). Restricting Topical Ocular
485 Chloramphenicol Eye Drop Use in the United States. Did We Overreact? *American*
486 *Journal of Ophthalmology* 156(3), 420-422.

- 487 [17] Lam, R.F., Lai, J.S.M., Ng, J.S.K., Rao, S.K., Law, R.W.K., and Lam, D.S.C.
488 (2002). Topical chloramphenicol for eye infections. *Hong Kong Medical Journal*, 8(1),
489 44-47.
- 490 [18] Titcomb, C.L. (2000). Topical ocular antibiotics: part 1. *The Pharmaceutical*
491 *Journal*, 264(7084), 298-301.
- 492 [19] Andrews, J.M. (2001). Determination of minimum inhibitory concentrations.
493 *Journal of Antimicrobial Chemotherapy*, 48, Suppl. S1, 5-16.
- 494 [20] Ghosal, K., Ranjan, A. and Bhowmik, B. (2014). A novel vaginal drug delivery
495 system: anti-HIV bioadhesive film containing abacavir. *Journal of Material Science:*
496 *Material Medicine*, 25(7), 1679-1689.
- 497 [21] Boateng, J.S., Mani, J., Kianfar, F. (2013). Improving drug loading of mucosal
498 solvent cast films using combination of hydrophilic polymers with amoxicillin and
499 paracetamol as model drugs. *BioMed Research International*, vol. 2013, Article ID
500 198137, 8 pages, 2013. doi:10.1155/2013/198137.
- 501 [22] Morales, J., McConville, J. (2011). Manufacture and characterization of
502 mucoadhesive buccal films. *European Journal of Pharmaceutics and*
503 *Biopharmaceutics*, 77(2), pp.187-199.
- 504 [23] Carvalho, F., Bruschi, M., Evangelista, R. and Gremiao, M. (2010).
505 Mucoadhesive drug delivery systems. *Brazilian Journal of Pharmaceutical Sciences*,
506 46(1), pp.1-19.
- 507 [24] Kumar, L., Kumar, P., Narayan, A. and Kar, M. (2013). Rietveld analysis of XRD
508 patterns of different sizes of nanocrystalline cobalt ferrite. *International Nano Letters*,
509 3(1), 8.
- 510 [25] Amar, A. (2012). Formulation and evaluation of controlled release ocular inserts of
511 betaxolol hydrochloride. *IOSR Journal of Pharmacy (IOSRPHR)*, 2(5), 34-38.

- 512 [26] Jethava, J. and Jethava, G. (2014). Design, formulation, and evaluation of novel
513 sustain release bioadhesive in-situ gelling ocular inserts of ketorolac tromethamine.
514 *International Journal of Pharmaceutical Investigation*, 4(4), 226.
- 515 [27] Jung, H.J., Abou-Jaoude, M., Carbia, B.E., Plummer, C., Chauhan, A. (2013).
516 Glaucoma therapy by extended release of timolol from nanoparticle loaded silicone-
517 hydrogel contact lenses, *Journal of Controlled Release*, 165(1), 82–89.
- 518 [28] Harris, M. and Chamberlain, M. (1978). Light Transmission of Hydrogel
519 Contact Lenses. *Optometry and Vision Science*, 55(2), 93-96.
- 520 [29] Rathod, K., Shah, C., and Shah, H. (2014). To optimize the effect of polymers
521 on matrix type transdermal patch of Trandolapril. *International Journal of*
522 *Pharmaceutical Research and Bioscience* 3(2), 540-554.
- 523 [30] Boateng, J.S., Stevens, H.N.E., Eccleston, G.M., Auffret, A.D., Humphrey,
524 M.J., Matthews, K.H. (2009). Development and mechanical characterization of
525 solvent-cast polymeric films as potential drug delivery systems to mucosal surfaces.
526 *Drug Development and Industrial Pharmacy*. 35(8), 986-996.
- 527 [31] Kianfar, F., Antonijevic, M., Chowdhry, B. and Boateng, J.S. (2011).
528 Formulation Development of a Carrageenan Based Delivery System for Buccal Drug
529 Delivery Using Ibuprofen as a Model Drug. *Journal of Biomaterials and*
530 *Nanobiotechnology*, 2, 582-595.
- 531 [32] Momoh, F., Boateng, J.S., Richardson, S., Mitchell, J., Chowdhry, B. (2015).
532 Development and functional characterization of alginate dressing as potential protein
533 delivery system for wound healing, *International Journal of Biological*
534 *Macromolecules*, 81, 137–150.

- 535 [33] Anshu, S., Jain, C. (2011). Solid dispersion: A promising technique to enhance
536 solubility of poorly water-soluble drug. *International Journal of Drug Delivery*, 3, 149-
537 170.
- 538 [34] Aburahma, M.H., Mahmoud A.A. (2011). Biodegradable ocular inserts for
539 sustained delivery of brimonidine tartarate: preparation and in vitro/in vivo
540 evaluation, *AAPS PharmSciTech*, 12(4), 1335–1347.
- 541 [35] Hehl E.M., Beck R., Luthard K., Guthoff R. (1999). Improved penetration of
542 aminoglycosides and fluoroquinolones into aqueous humour of patients by means of
543 Acuvue contact lenses. *European Journal of Clinical Pharmacology*, 55, 317-323.
- 544 [36] Schultz CL, Mint JM. 2002. Drug Delivery system for antiglaucomatous
545 medication. US Patent 6 410 045, 25 June.
- 546 [37] Gulsen, D., Chauhan, A. (2004). Ophthalmic drug delivery through contact
547 lenses. *Investigative Ophthalmology and Visual Science*, 45(7), 2342-2347.
- 548
- 549
- 550
- 551
- 552

553 **Figure legends**

554 **Figure 1:** Digital images of optimum films formulated (a) BLK HPMC-EUD-PEG (b) BLK
555 HPMC-PEG-EUD-PEG (c) DL HPMC-CHF-EUD-PEG (d) DL HPMC-PEG-CHF-EUD-
556 PEG.

557

558 **Figure 2:** (a) Tensile profiles showing average (\pm SD, $n = 3$) % elongation at break, tensile
559 strength and elastic modulus for BLK (HPMC-EUD-PEG & HPMC-PEG-EUD-PEG) and
560 DL (HPMC-CHF-EUD-PEG & HPMC-PEG-CHF-EUD-PEG) films and (b) Mucoadhesion
561 profiles (\pm SD, $n = 3$) showing average detachment force for both BLK and DL films.

562

563 **Figure 3:** SEM images for (a) pure CHF, (b) HPMC layer of BLK HPMC-EUD-PEG films
564 and EUD layer of BLK HPMC-EUD-PEG; bi-layer films [(the SEM images of DL films
565 containing CHF are shown in supplementary data section (Figure A1)]

566

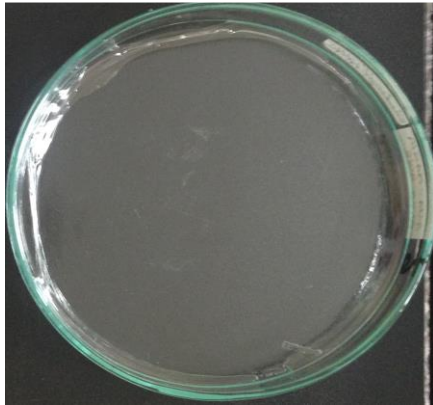
567 **Figure 4:** DSC thermograms obtained for (a) pure CHF and (b) BLK (HPMC-EUD-PEG &
568 HPMC-PEG-EUD-PEG) and DL (HPMC-CHF-EUD-PEG & HPMC-PEG-CHF-EUD-PEG)
569 films.

570

571 **Figure 5:** (a) XRD diffractograms for BLK (HPMC-EUD-PEG & HPMC-PEG-EUD-PEG)
572 and DL (HPMC-CHF-EUD-PEG) films and (b) EDX results for CHF and DL HPMC-PEG-
573 CHF-EUD-PEG film.

574

575 **Figure 6:** (a) Swelling profiles comparing swelling capacity for BLK (HPMC-EUD-PEG &
576 HPMC-PEG-EUD-PEG) and DL (HPMC-CHF-EUD-PEG & HPMC-PEG-CHF-EUD-PEG)
577 bi-layered films and (b) *In vitro* drug dissolution profiles (\pm SD, $n = 3$) of (a) DL HPMC-
578 CHF-EUD-PEG and DL HPMC-PEG-CHF-EUD-PEG films.



(a) HPMC-EUD-PEG



(b) HPMC-PEG-EUD-PEG

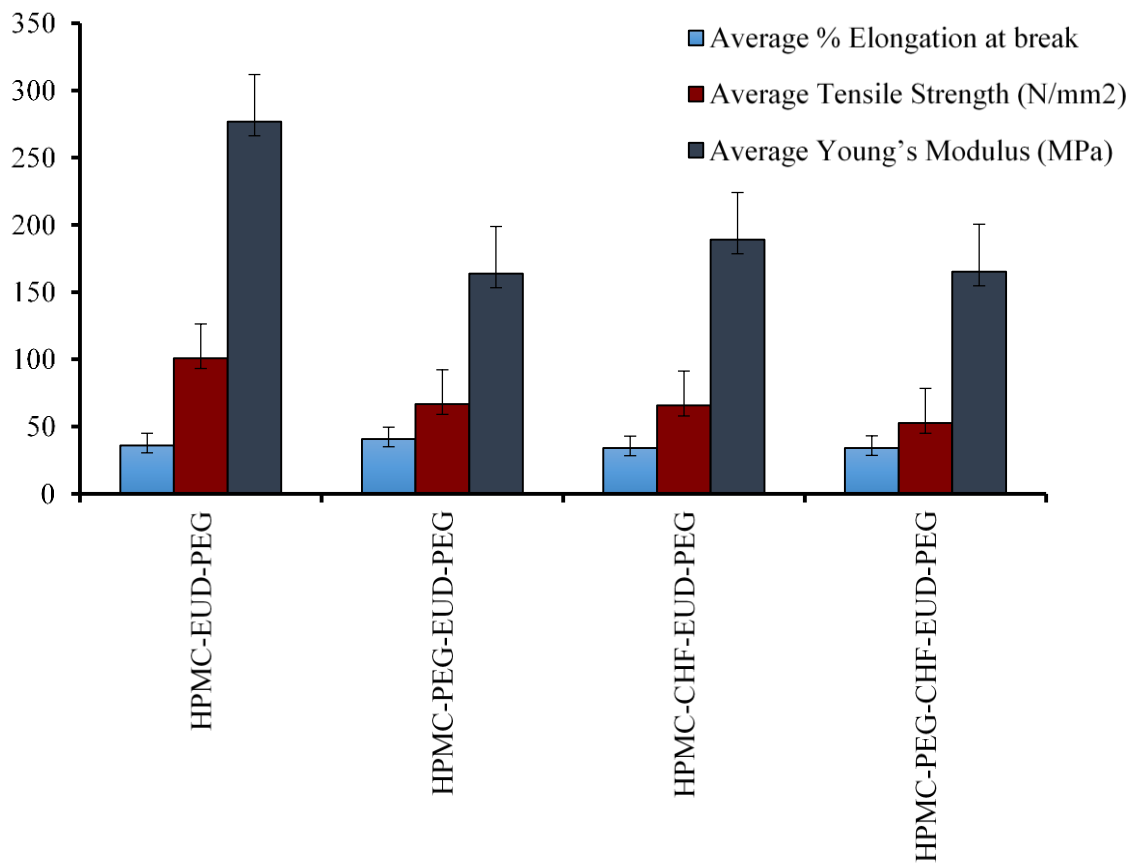


(c) HPMC-CHF-EUD-PEG

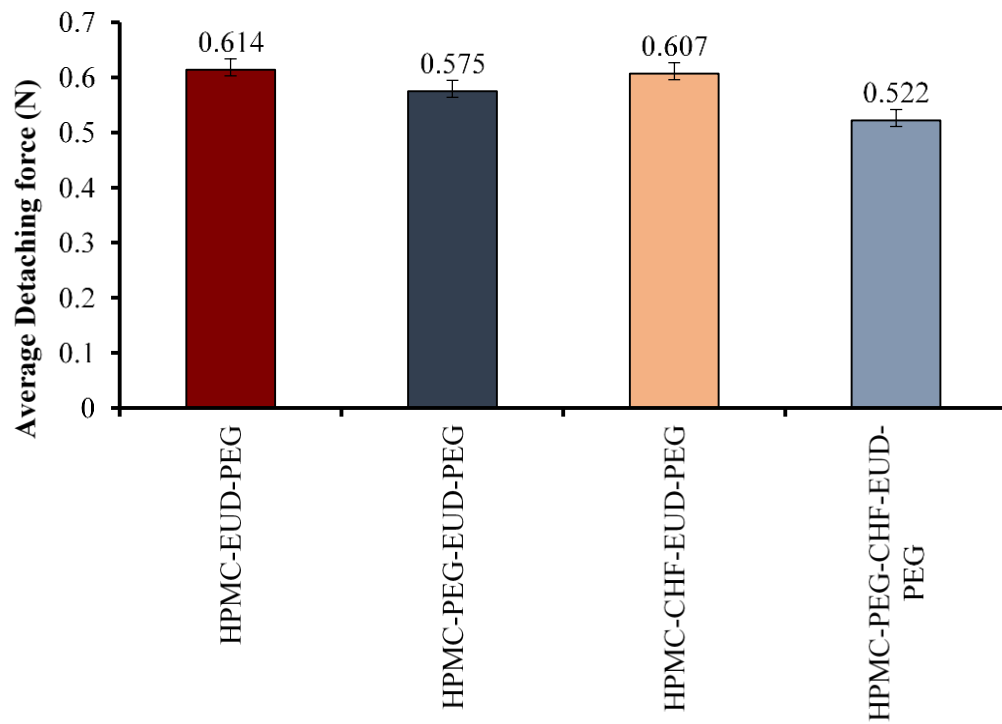


(d) HPMC-PEG-CHF-EUD-PEG

Figure 1

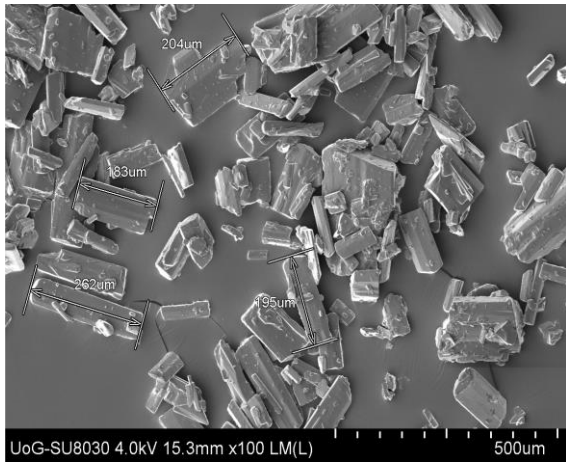


(a)

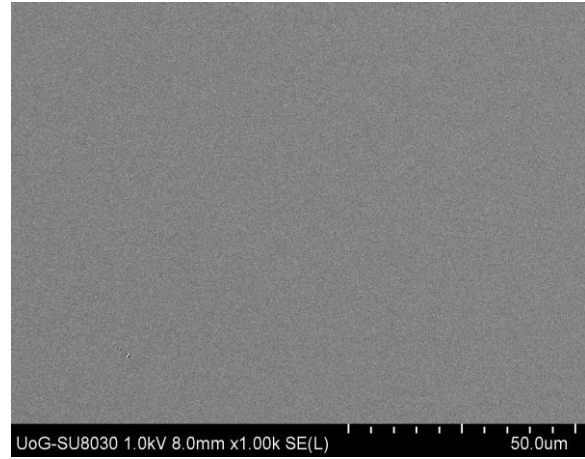


(b)

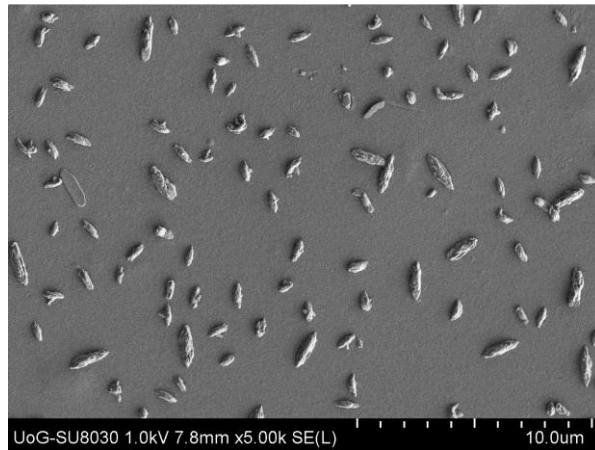
Figure 2



(a) CHF

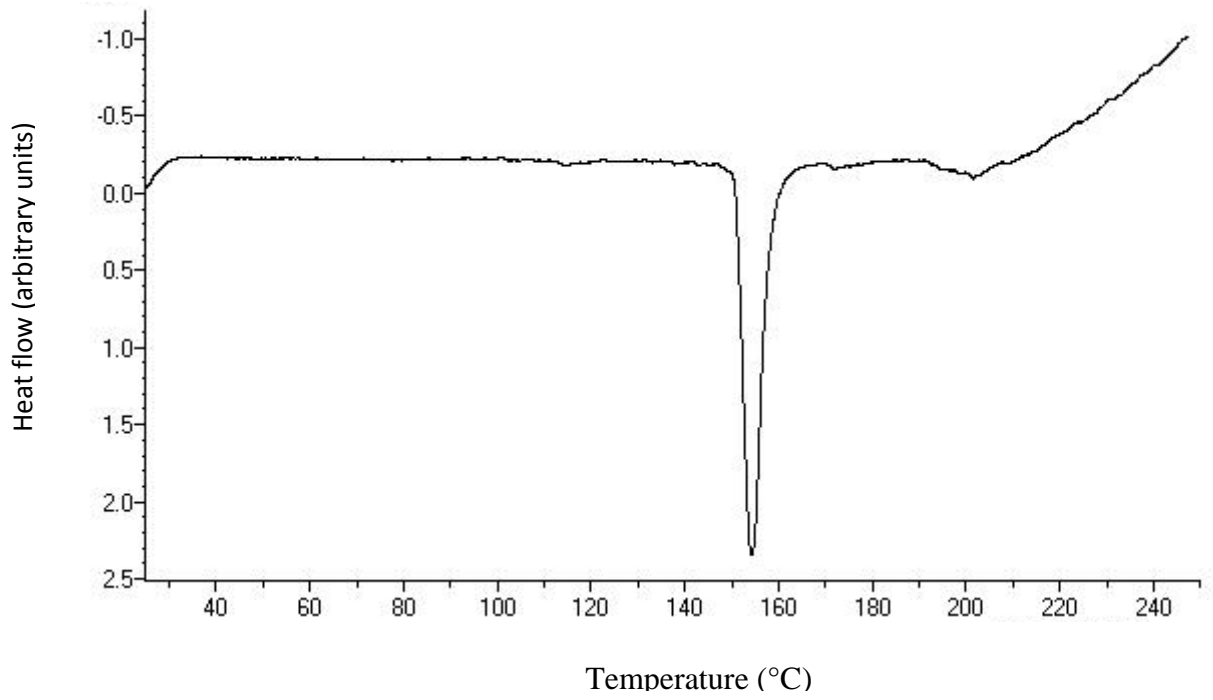


(b) HPMC-EUD-PEG film: EUD layer

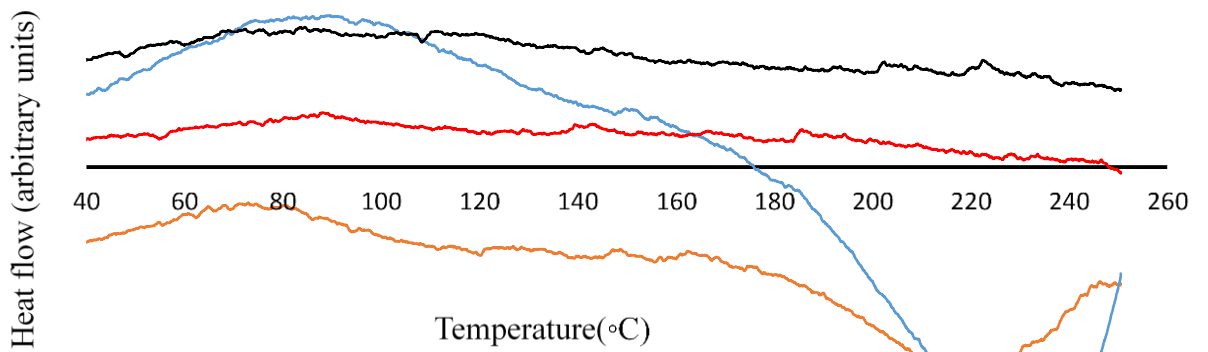


(c) HPMC-EUD-PEG film: HPMC layer

Figure 3



(a)



— BLK HPMC-EUD-PEG

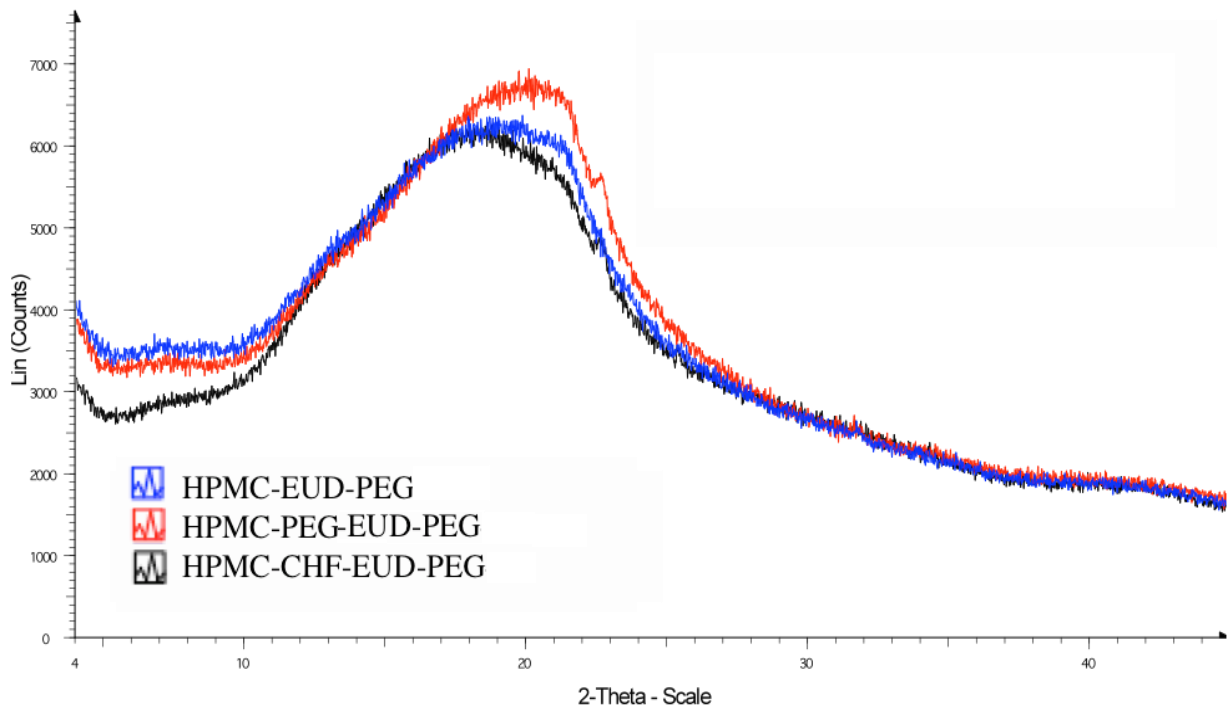
— BLK HPMC-PEG-EUD-PEG

— HPMC-CHF-EUD-PEG

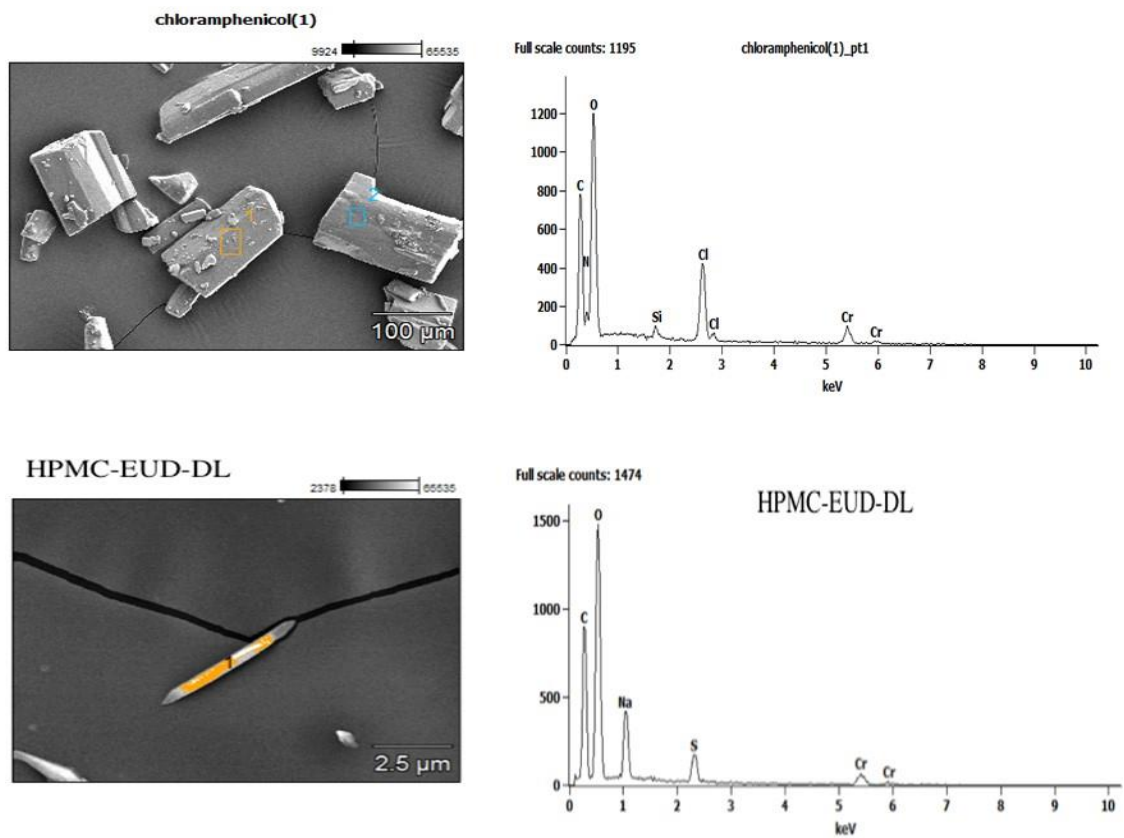
— DL HPMC-CHF-PEG-EUD-PEG

(b)

Figure 4

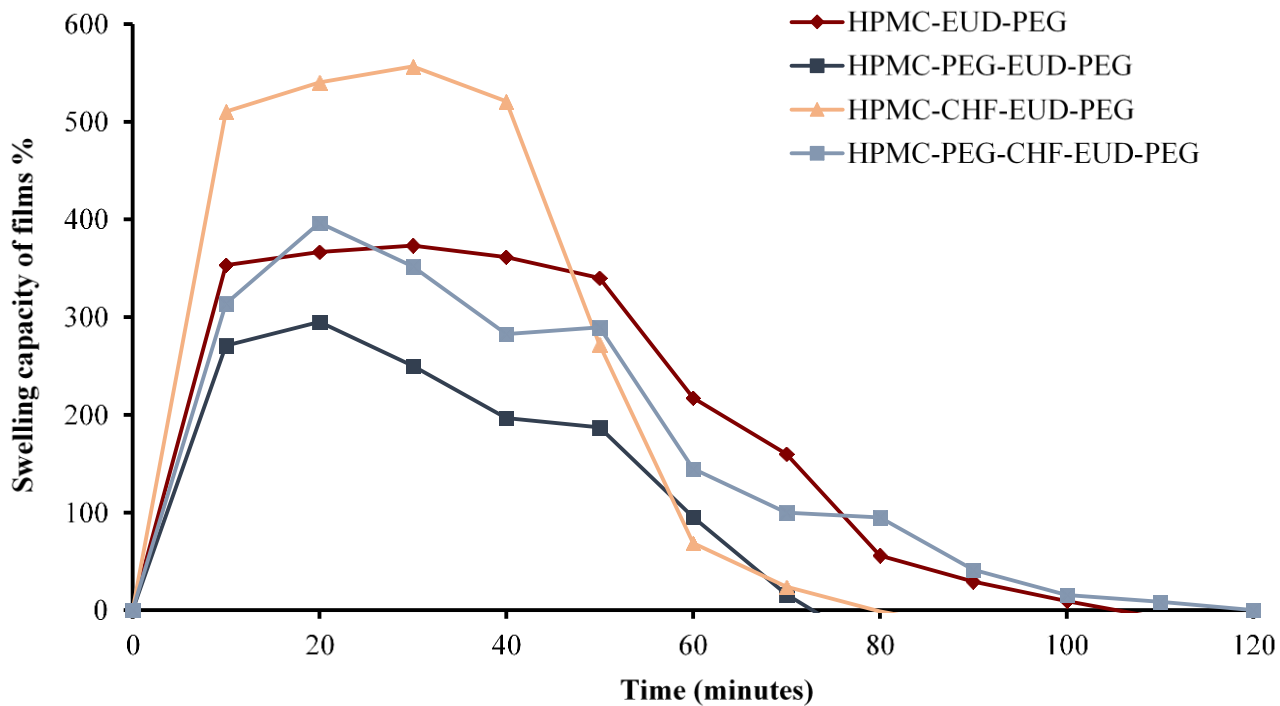


(a)

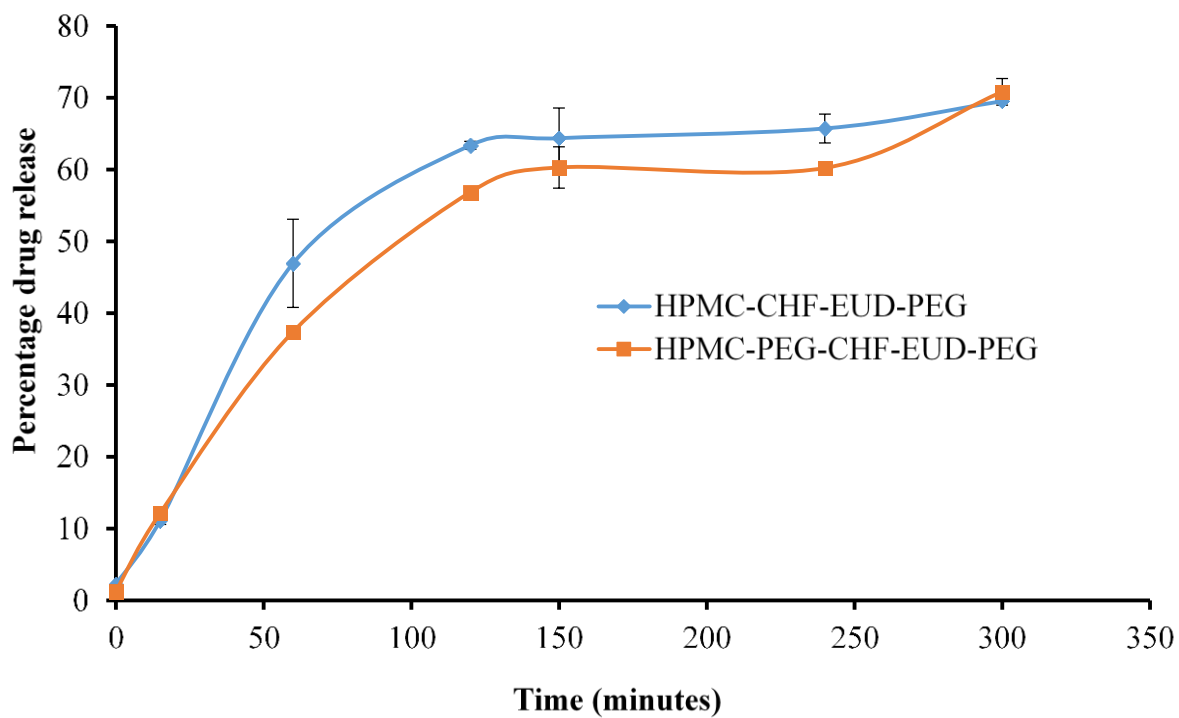


(b)

Figure 5



(a)



(b)

Figure 6

584

585